Cosmogenic nuclide dating of *Sahelanthropus tchadensis* and *Australopithecus bahrelghazali*: Mio-Pliocene hominids from Chad

Anne-Elisabeth Lebatard*†, Didier L. Bourlès†‡, Philippe Duringer§, Marc Jolivet¶, Régis Braucher†, Julien Carcaillet‖, Mathieu Schuster*, Nicolas Arnaud¶, Patrick Monié¶, Fabrice Lihoreau, Andossa Likius††, Hassan Taisso Mackaye††, Patrick Vignaud*, and Michel Brunet*‡,‡‡**

*Institut International de Paléoprimatologie, Paléontologie Humaine: Evolution et Paléoenvironnements, Unité Mixte de Recherche Centre National de la Recherche Scientifique 6046, Faculté des Sciences, Université de Poitiers, 40 Avenue du Recteur Pineau, 86022 Poitiers Cedex, France; †Centre Européen de Recherche et d'Enseignement des Géosciences de l'Environnement, Unité Mixte de Recherche, Centre National de la Recherche Scientifique 6635, Université Paul Cézanne, Plateau de l'Arbois, 13545 Aix-en-Provence Cedex 04, France; §Ecole et Observatoire des Sciences de la Terre, Centre de Géochimie de la Surface, Centre National de la Recherche Scientifique, Unité Mixte de Recherche 7517, Institut de Géologie, Université Louis Pasteur, 1 Rue Blessig, 67084 Strasbourg Cedex, France; ¶Laboratoire de Géosciences de Montpellier, Unité Mixte de Recherche, Centre National de la Recherche Scientifique 5243 and **Laboratoire de Phylogénie, Paléobiologie, et Paléontologie, Unité Mixte de Recherche, Centre National de la Recherche Scientifique 5554, Université Montpellier II, Cc 060, 5 Place Eugène Bataillon, 34095 Montpellier Cedex 05, France; ‖Laboratoire de Géodynamique des Chaînes Alpines, Maison des Géosciences, Unité Mixte de Recherche, Centre National de la Recherche Scientifique 5025, Université J. Fourier, 1381 Rue de la Piscine, 38400 Saint Martin d'Hères, France; ††Département de Paléontologie, Faculté des Sciences Exactes et Appliquées, Université de N'Djamena, BP1117 N'Djamena, Chad; and ‡‡Chaire de Paléontologie Humaine, Collège de France, 11 Place Marcelin Berthelot, 75231 Paris Cedex 05, France

Edited by Thure E. Cerling, University of Utah, Salt Lake City, UT, and approved January 22, 2008 (received for review August 24, 2007)

Ages were determined at two hominid localities from the Chad Basin in the Djurab Desert (Northern Chad). In the Koro Toro fossiliferous area, KT 12 locality (16°00′N, 18°53′E) was the site of discovery of *Australopithecus bahrelghazali* (Abel) and in the Toros-Menalla fossiliferous area, TM 266 locality (16°15′N, 17°29′E) was the site of discovery of *Sahelanthropus tchadensis* (Toumaï). At both localities, the evolutive degree of the associated fossil mammal assemblages allowed a biochronological estimation of the hominid remains: early Pliocene (3–3.5 Ma) at KT 12 and late Miocene (≈7 Ma) at TM 266. Atmospheric ^{10}Be, a cosmogenic nuclide, was used to quasicontinuously date these sedimentary units. The authigenic ^{10}Be/^{9}Be dating of a pelite relic within the sedimentary level containing Abel yields an age of 3.58 ± 0.27 Ma that points to the contemporaneity of *Australopithecus bahrelghazali* (Abel) with *Australopithecus afarensis* (Lucy). The 28 ^{10}Be/^{9}Be ages obtained within the anthracotheriid unit containing Toumaï bracket, by absolute dating, the age of *Sahelanthropus tchadensis* to lie between 6.8 and 7.2 Ma. This chronological constraint is an important cornerstone both for establishing the earliest stages of hominid evolution and for new calibrations of the molecular clock.

beryllium-10 | absolute dating | hominid site | Abel | Toumaï

We determined authigenic ^{10}Be/^{9}Be ages at two hominid localities in the Chad Basin (Djurab Desert of northern Chad). The focus of this study was the Toros-Menalla (TM) fossiliferous area, where *Sahelanthropus tchadensis* (Toumaï) was unearthed. Localities investigated in this area include TM 266 and TM 254 (Fig. 1). The Kollé (KL), Kossom Bougoudi (KB), and Koro Toro (KT) fossiliferous areas were specifically studied to calibrate the authigenic ^{10}Be/^{9}Be dating method by direct comparison with biochronological estimations of co-located mammalian assemblages. Fossiliferous localities investigated in these areas were KL, KB 1, and KT 12 (Fig. 2). KT 12 (16°00′N, 18°53′E) is the site of *Australopithecus bahrelghazali* (Abel).

Discoveries at the TM 266 locality (16°15′N, 17°29′E) in the Toros-Menalla fossiliferous area in northern Chad of notably a nearly complete cranium, holotype of *Sahelanthropus tchadensis* (Toumaï) (1, 2) have changed substantially the understanding of early human evolution in Africa (1–4). The sedimentary unit from which Toumaï was unearthed was named the anthracotheriid unit (A.U.) after a very common, large anthracotheriid, *Libycosaurus petrochii* (5) that it contained. The A.U. also contains a mammalian fauna that includes taxa that are more primitive than the Lukeino fauna [Kenya, dating from 6 Ma ago (6)] and similar to the fauna from the lower Nawata Formation of Lothagam [Kenya, 6.5–7.4 Ma ago (7)]. Recent investigations conducted at another locality, TM 254, ≈18 km west of the *Sahelanthropus tchadensis* TM 266 locality, reveal the presence of a 30-cm thick gray-blue ash tuff layer exclusively made up of volcanic ash. This ash tuff layer, a potential target for ^{40}Ar/^{39}Ar dating, is not exposed at TM 266; therefore, 20 intermediate geological sections between TM 266 and TM 254 have been documented to determine its stratigraphic position within the A.U. The sections are uniform in facies across the transect. The base of the mapped sections consists of a well developed, thick, aeolian facies (8). The middle part (e.g., the A.U.) is composed of poorly cemented sand and argillaceous sandstone alternation characterized by dense networks of root tubules/root molds (palaeosols) and termite nests (9, 10). The top records extensive lacustrine facies (Fig. 1). Geological correlations between TM 266 and TM 254 are firmly supported by the same continuity of stratigraphy between the sites, reflecting a similar environment and climate change history (5). The uniform stratigraphy at the TM localities allowed us to use absolute ages from both TM 266, where Toumaï was discovered, and TM 254 to assign an age to Toumaï. It was hoped that the tephra layer would contain material datable by the ^{40}Ar/^{39}Ar method, but petrographic study demonstrated that this is not the case by using currently available techniques. The glass shards present were very small (<1 mm), contained many fluid inclusions (mainly gas bubbles that may contain ^{36}Cl), and their surfaces were covered with K-rich micas. All of these properties precluded their suitability for ^{40}Ar/^{39}Ar dating.

Being unable to apply ^{40}Ar/^{39}Ar dating, we explored the possibility that the depositional environment may be favorable for the application of cosmogenic ^{10}Be produced in the atmosphere to

Author contributions: D.L.B., P.V., and M.B. designed research; A.-E.L., D.L.B., P.D., M.J., R.B., J.C., N.A., P.M., F.L., A.L., and H.T.M. performed research; A.-E.L., D.L.B., M.J., J.C., N.A., and P.M. contributed new reagents/analytic tools; A.-E.L., D.L.B., P.D., M.J., R.B., M.S., N.A., and P.M. analyzed data; and A.-E.L., D.L.B., P.D., M.J., M.S., N.A., P.V., and M.B. wrote the paper.

The authors declare no conflict of interest.

This article is a PNAS Direct Submission.

Freely available online through the PNAS open access option.

‡To whom correspondence may be addressed. E-mail: bourles@cerege.fr or michel.brunet@univ-poitiers.fr.

© 2008 by The National Academy of Sciences of the USA

www.pnas.org/cgi/doi/10.1073/pnas.0708015105

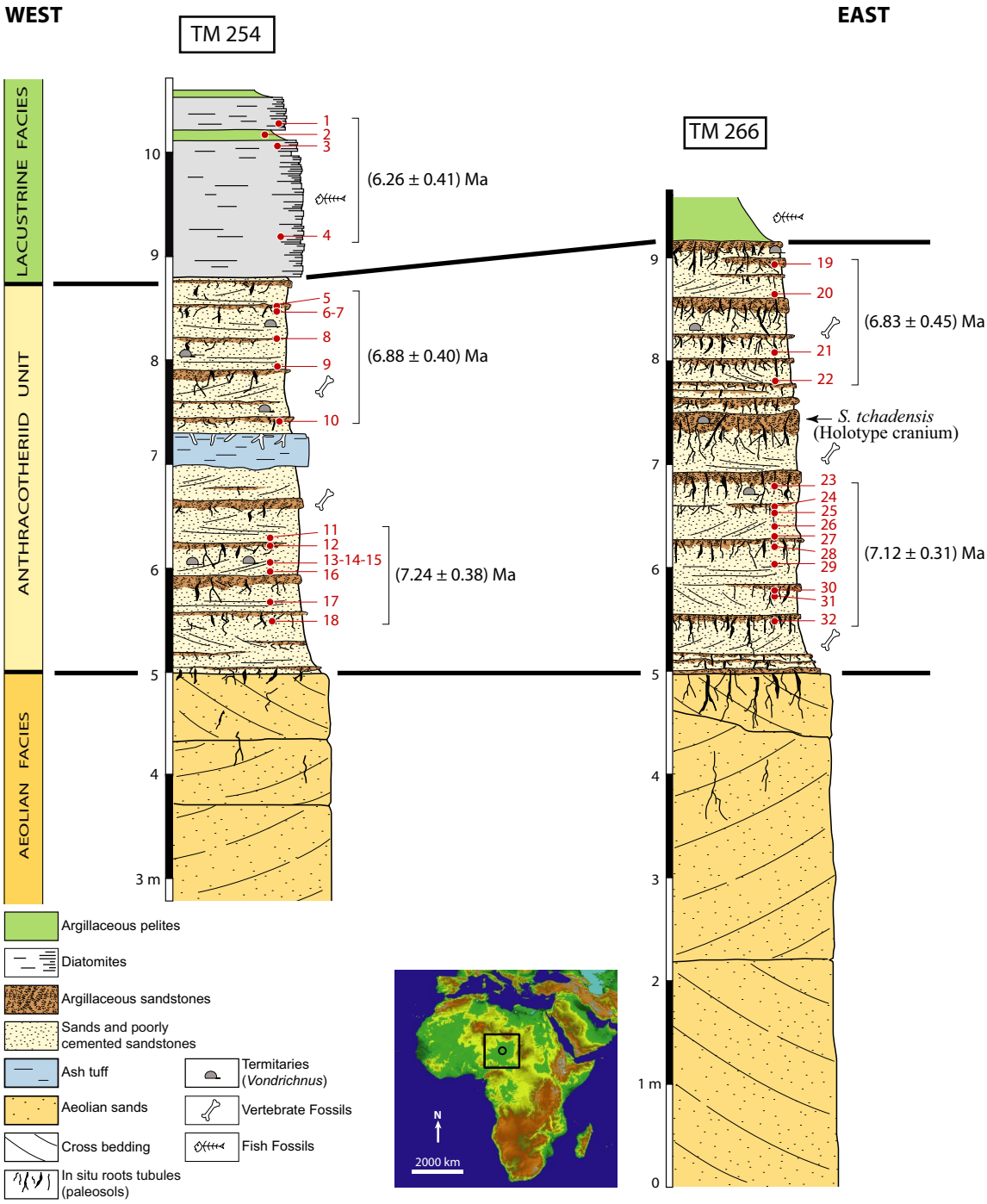

Fig. 1. Stratigraphic columns and beryllium ages of TM 254 and TM 266 (*Sahelanthropus tchadensis* locality, Toros-Menalla, Upper Miocene, Northern Chad). (The circle on the localization map indicates the studied area; red numbers, number of the sample in Table 2.) The Toumaï cranium is precisely located in the TM 266 section.

quascontinuously date the A.U. To this end, 32 ^{10}Be/^{9}Be ages within the A.U. and the overlying lacustrine facies were determined.

Fundamentals of the ^{10}Be/^{9}Be Dating Method

The dating method used here is similar in many ways to ^{14}C dating. Like ^{14}C, ^{10}Be is mainly produced in the atmosphere, but through spallation reactions on oxygen (O) and nitrogen (N) rather than via a (neutron, proton) reaction on ^{14}N as is the case for ^{14}C. The particle-reactive ^{10}Be adsorbs on aerosols and is rapidly transferred to the surface of the Earth in soluble form by precipitation (11). If deposited in an aqueous environment, ^{10}Be is ultimately removed from water on settling particles and deposited in marine and lacustrine sediments. If deposited in a continental setting, ^{10}Be associates with continental particles, where it decays with a half-life of ≈1.4 million years. This opens up the possibility to date sedimentary deposits in the range of 0.2 to 14 Ma.

Much as is the case with ^{14}C and its daughter ^{14}N, it is not possible to determine an age by measuring the ratio between the parent isotope, ^{10}Be, and its daughter product, radiogenic ^{10}B, which is undistinguishable from common boron. This is unlike most other

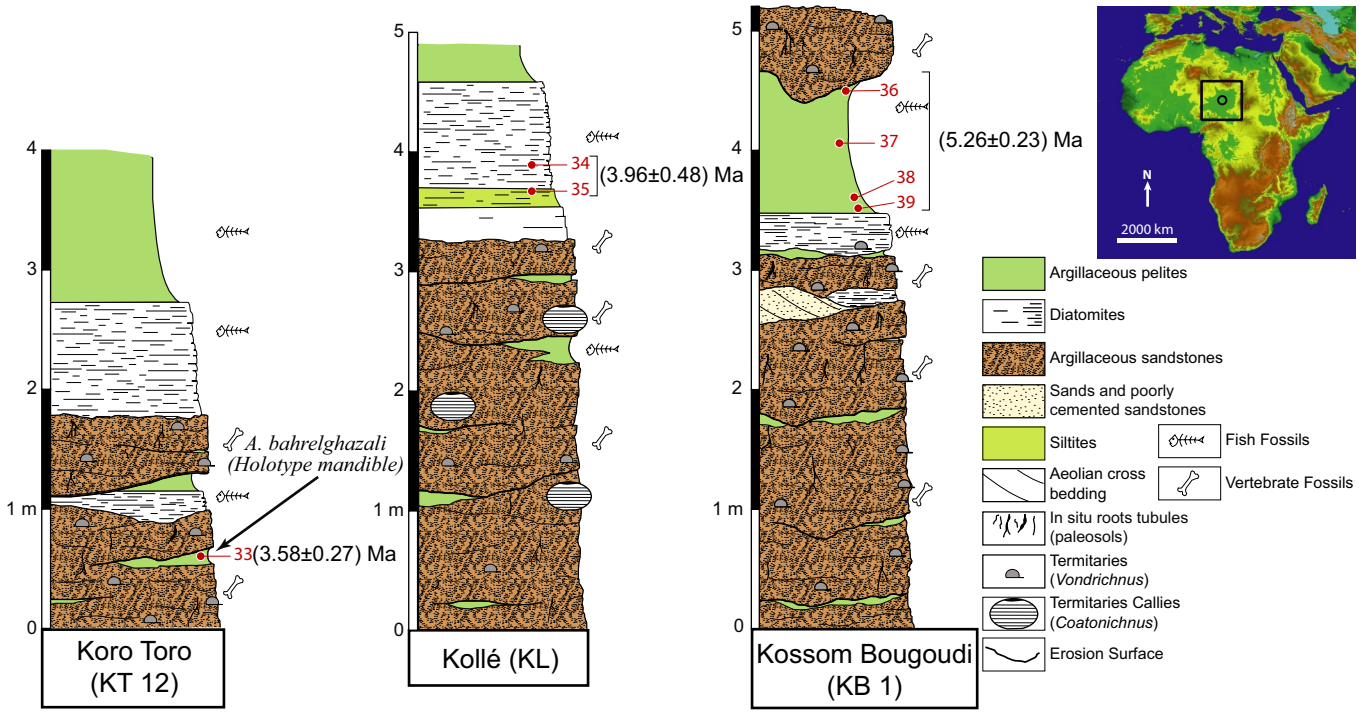

Fig. 2. Stratigraphic columns and beryllium ages of KT 12 (*Australopithecus bahrelghazali* locality, Koro Toro, Early Pliocene, Northern Chad), KL and KB 1. (The circle on the localization map indicates the studied area; red numbers, number of the sample in Table 2). The *Australopithecus bahrelghazali* holotype is precisely located in KT 12 section.

radiochronological methods (U-Th, Rb-Sr, Sm-Nd, K-Ar, Lu-Hf, Re-Os, etc.) that rely on parent–daughter ratios to determine ages. In addition, because the absolute ^{10}Be concentration depends also on parameters such as the scavenging efficiency and the specific surface area of the sedimentary particles, it cannot be used directly to determine an age. It is first necessary to find some method of normalizing ^{10}Be concentrations that accounts for these processes. Stable ^{9}Be is a good candidate for such a normalizing species. Although ^{10}Be and stable ^{9}Be have different sources [^{10}Be is from cosmogenic production in the atmosphere, and ^{9}Be is from detrital input, of which a small fraction is dissolved (12, 13)], it has been shown that, in suitable instances, the dissolved beryllium isotopes are homogenized before deposition and that their ratio is a useful chronologic tool. To use ^{9}Be as a normalizing species for the decay of ^{10}Be, a method is needed to extract only that portion of the beryllium that originated from solution, i.e., the authigenic Be that is adsorbed on particles and/or precipitated directly from solution. Sequential leaching procedures have been developed to selectively extract this authigenic component for dating purposes (14). It has effectively been demonstrated in marine systems that the ^{10}Be/^{9}Be ratio of the resulting leachate represents the ^{10}Be/^{9}Be ratio of soluble beryllium at the time of deposition (14).

Focusing on the authigenic component, there are two essential requirements in order that the decay of ^{10}Be may be used for dating according to the following equation: $N_{(t)} = N_0 e^{-\lambda t}$ (where $N_{(t)}$ is the measured ^{10}Be/^{9}Be authigenic ratio, N_0 is the initial authigenic ratio, λ is the radioactive decay constant for ^{10}Be, and t is the age of the sediments). The first is that authigenic $(^{10}\text{Be}/^{9}\text{Be})_0$ can be accurately estimated, and the second is that the selected samples must have remained "closed" to entry or loss of the cosmogenic isotope and its normalizing isotope. If these requirements are met, then ^{10}Be/^{9}Be will decrease with time according to the above equation. This is analogous to the decrease in the ^{14}C/^{12}C ratio with time in the radiocarbon dating system.

C-14 has a universal initial ^{14}C/^{12}C ratio (15) because it is rapidly oxidized to form gaseous $^{14}CO_2$ and is then globally homogenized with the natural carbon isotopes during its 7 to 8 years residence time in the atmosphere. On the other hand, cosmogenic ^{10}Be and its normalizing parameter, terrigenous authigenic ^{9}Be, have different sources. The initial authigenic ^{10}Be/^{9}Be ratio is, therefore, not expected to be globally homogeneous but may be influenced by the proximity to continental sources of various strength that may influence the flux of ^{9}Be input to the sampled area. Thus ^{10}Be/^{9}Be may vary significantly from one environmental context to another. It has been shown that values of authigenic ^{10}Be/^{9}Be reported for surface marine sediments (14, 16), for top surfaces (or extrapolated to zero age) of Fe-Mn deposits (17–23), for present-day deep waters in the Atlantic, Pacific, Indian Ocean, and Mediterranean Sea central basins and margins (13, 24–30) mostly range between 0.5×10^{-8} to 30×10^{-8} and indeed evidence significant spatial variations. Similarly, studies conducted on continental sediments show contrasting initial authigenic ^{10}Be/^{9}Be ratios that vary, for example, from between 1.55×10^{-10} and 9.58×10^{-10} in tropical riverine suspended sediments (13) to 3.5×10^{-8} on a New Zealand loess–paleosol sequence (31). Such large variations of the initial continental authigenic ^{10}Be/^{9}Be ratio can be expected considering that in continental systems, the two major processes affecting the aqueous geochemistry of beryllium are dissolution from rocks and uptake onto particles (13). The initial authigenic ^{10}Be/^{9}Be ratio thus depends both on the lithology of the region drained and on the partitioning between solid and aqueous phases. The magnitude of the latter process is tightly linked to the geochemical and the hydrogeological contexts at the time of the sedimentary deposition. To apply the radioactive decay equation described above, it is thus essential to know the regional initial authigenic ^{10}Be/^{9}Be ratio. The best way to do this is to measure recent samples deposited in an environmental context similar to that in which the sediments of interest have been deposited, that is, in our case, during periods of major lacustrine extension.

Lacustrine diatoms built their silicate frustules from dissolved elements and thus are an ideal substrate for registering the dissolved isotopic ratio of ^{10}Be/^{9}Be at the time that they were alive. To

Table 1. N_0 initial authigenic $^{10}Be/^{9}Be$ ratio calculation from four Holocene Lake Mega-Chad diatomite samples

Sample	S. unit	Age	Lithology	Sample depth,* m	Natural $[^{10}Be]/[^{9}Be]$,† $\times 10^{-8}$
TOD1	Lacustrine	Holocene	Diatomite	0.20	2.72 ± 0.25
TOD1	Lacustrine	Holocene	Diatomite	0.30	2.46 ± 0.14
TOD2	Lacustrine	Holocene	Diatomite	1.00	2.66 ± 0.16
TOD2	Lacustrine	Holocene	Diatomite	2.40	2.44 ± 0.19

S., sedimentary.
*Mean square of the weighted deviate, 0.55.
†Weighted mean ± SD: $2.54 \times 10^{-8} \pm 8.75 \times 10^{-10}$; N_0, $2.54 \times 10^{-8} \pm 0.09 \times 10^{-8}$.

establish the regional initial $^{10}Be/^{9}Be$ ratio (N_0) for the system studied here, we measured selected diatomites deposited in the north part of the basin during the last Holocene expansion of Lake Mega-Chad (32) (≈7 to 4.4 ka BP), obtaining a value of $(2.54 \pm 0.09) \times 10^{-8}$ (Table 1).

Although the initial $^{10}Be/^{9}Be$ ratio recorded in authigenic Mn deposits is reported to have remained constant to ± 6% over the past ≈8 Ma (22), much like the atmospheric $^{14}C/^{12}C$ ratio, the initial authigenic $^{10}Be/^{9}Be$ ratio is sensitive to variations of the geomagnetic field intensity and the solar activity that effect ^{14}C and ^{10}Be production in a similar fashion. To evaluate potential past variations of the initial authigenic $^{10}Be/^{9}Be$ ratio, we used a method similar to that developed over several decades to build the ^{14}C calibration curve, that is we compared the calculated authigenic $^{10}Be/^{9}Be$ ages with ages obtained by independent methods.

The authigenic $^{10}Be/^{9}Be$ ages were calculated by using the previously determined initial ratio and the recently reevaluated ^{10}Be half-life of $(1.36 \pm 0.07) \times 10^{6}$ years (33). Weighted mean ^{10}Be ages were calculated with the inverse-variance weighted mean when more than two samples are considered and with the weighted mean when only two are. This as well as the associated uncertainties is fully discussed in the Materials and Methods section. In this first attempt of calibration in a continental context, the calculated authigenic $^{10}Be/^{9}Be$ ages obtained in or close to the fossiliferous levels were compared with the ages estimated by using the evolutive degree of fossil mammal assemblages. This is the sole independent dating method available in the study area which, until now is devoid of volcanic deposits appropriate for isotopic and/or radiogenic dating methods.

Mammal fossil assemblages unearthed from argillaceous sandstone levels at Koro Toro (KT 12) and Kollé (KL) allowed a biochronological estimation of their deposition age of 3–3.5 Ma and 4–5 Ma (3–4, 34), respectively. The green pelite level sampled at Koro Toro yields an authigenic $^{10}Be/^{9}Be$ age of 3.58 ± 0.27 Ma, whereas at Kollé, the sampled siliceous (diatomites and siltites) levels yield a mean age value of 3.96 ± 0.48 Ma (Table 2 and Fig. 2). This is remarkably consistent with the mammal faunal age estimations, considering that at Koro Toro, the level sampled for this study is within the level from which the fauna and the *Australopithecus bahrelghazali* holotype were unearthed, whereas at Kollé, the sampled levels overlay the fossiliferous level.

At Kossom Bougoudi (KB 1), the fauna is older than that from Kollé, with an age close to the Mio-Pliocene boundary that is ≈5.3 Ma (5, 35). The authigenic $^{10}Be/^{9}Be$ ages obtained from four samples taken in a green pelite level (Table 2) interbedded within the discussed fossiliferous poorly cemented sandstones yield an inverse-variance weighted mean age of 5.26 ± 0.29 Ma, again remarkably consistent with the biochronological estimation.

The demonstrated systematic strong agreement between the biochronological estimations and the calculated authigenic $^{10}Be/^{9}Be$ ages strongly suggests not only that the initial authigenic $^{10}Be/^{9}Be$ ratio can be constrained by using appropriate Holocene deposits but also that this ratio remained relatively constant over the studied time period, confirming the conclusion of the work of Ku *et al.* (22) and suggesting thus that the temporal resolution of the extracted authigenic phases allows smoothing the production rate changes.

In addition, the validity of the calibration of the authigenic $^{10}Be/^{9}Be$ ages based on an initial authigenic ratio determined from sediments deposited in Holocene Lake Mega-Chad demonstrates that the sedimentary levels (clays, diatomites, argillites, siltites, and poorly cemented sandstones) deposited in the Chad Basin during wet periods (5) accompanied by major lacustrine extension in an area otherwise characterized by a recurrent desert climate since at least 8 Ma (8) have remained closed to gain or loss of beryllium other than by radioactive decay despite cycles of inundation and desiccation.

Results

Having demonstrated that the two prerequisites necessary to apply the radioactive decay dating method are met in the studied area, we measured authigenic $^{10}Be/^{9}Be$ ratio of 32 samples from the TM 254 and TM 266 sections. By using the previously discussed initial ratio and the recently reevaluated ^{10}Be half-life of $(1.36 \pm 0.07) \times 10^{6}$ years (33), these ratios yielded ages ranging from 5.39 ± 0.92 to 8.67 ± 1.11 Ma. Weighted mean ^{10}Be ages were then calculated by using an inverse-variance weighted mean. Associated uncertainties are fully discussed in *Materials and Methods*. More specifically, the TM 254 lacustrine facies yielded a weighted mean authigenic $^{10}Be/^{9}Be$ age of 6.26 ± 0.41 Ma (Table 2 and Fig. 1). The section of the A.U. above the ash tuff layer at TM 254 yielded a weighted mean authigenic $^{10}Be/^{9}Be$ age of 6.88 ± 0.40 Ma, whereas the section of this layer below the ash tuff layer yielded a weighted mean authigenic $^{10}Be/^{9}Be$ age of 7.24 ± 0.38 Ma. In section TM 266, ages calculated for the two levels bracketing the *Sahelanthropus tchadensis* cranium level were 6.83 ± 0.45 Ma for the overlying level and 7.12 ± 0.31 Ma for the underlying level.

Because these data demonstrate that the deposition of the A.U. from which Toumaï was unearthed is synchronous and geologically instantaneous (considering the uncertainties associated to the dating methods) in both TM 266 and TM 254, all of the 28 samples from the A.U. were used to determine the inverse-variance weighted mean age of this sedimentary unit, the associated mean square of weighted deviates being 0.36 (see *Materials and Methods*). This yields an age of 7.04 ± 0.18 Ma for *Sahelanthropus tchadensis*.

Discussion

The data presented here demonstrate the accuracy of the measured authigenic $^{10}Be/^{9}Be$ ages through comparison with biochronological estimations based on the evolutive degree of fossil mammal lineages. This study shows that in favorable environments atmospheric cosmogenic ^{10}Be normalized to the dissolved fraction of its stable isotope, ^{9}Be, can be used as a dating tool for continental sedimentary deposits over the time period 0.2 to ≈7 Ma. The arid environment punctuated by wet periods during which a large shallow lake formed both provided Holocene sediments with which to determine the $^{10}Be/^{9}Be$ initial and preserved the older sediments in an environment that guaranteed their closed-system behavior.

ANTHROPOLOGY

Table 2. Authigenic $^{10}Be/^{9}Be$ ratio and age for 39 sediment samples from four Lower Pliocene to Upper Miocene sampling localities

Section	Height, m	Sedimentary unit	Lithology	$[^{10}Be]/[^{9}Be]$, $\times 10^{-10}$	Age, yr $\times 10^{6}$	Ref.	Mean age, yr $\times$ 10^{6} (MSWD)
KT 12*	0.6	Lacustrine	Pelites	41.06 ± 1.77	3.58 ± 0.27	33	
KL	4	Lacustrine	Diatomite	32.67 ± 2.08	4.03 ± 0.36	34	
KL	3.6	Lacustrine	Pelites	35.08 ± 1.86	3.89 ± 0.32	35	
							3.96 ± 0.48†
KB 1	4.7	Lacustrine	Pelites	23.46 ± 1.33	4.68 ± 0.39	36	
KB 1	4.2	Lacustrine	Pelites	17.53 ± 0.93	5.25 ± 0.43	37	
KB 1	3.7	Lacustrine	Pelites	11.19 ± 0.76	6.13 ± 0.56	38	
KB 1	3.4	Lacustrine	Pelites	15.05 ± 0.97	5.55±0.49	39	
							5.26 ± 0.29‡ (1.64)
TM 254	10.2	Lacustrine	Diatomite	10.65 ± 0.90	6.23 ± 0.65	1	
TM 254	10.1	Lacustrine	Pelites	11.74 ± 1.22	6.04 ± 0.73	2	
TM 254	10	Lacustrine	Diatomite	13.66 ± 2.90	5.74 ± 1.27	3	
TM 254	9.1	Lacustrine	Diatomite	7.31 ± 0.86	6.96 ± 0.92	4	
							6.26 ± 0.41‡ (0.28)
TM 254	8.5	A.U.	Argil. sandst.	16.36 ± 2.60	5.39 ± 0.92	5	
TM 254	8.4	A.U.	Sandstones	7.68 ± 0.76	6.87 ± 0.80	6	
TM 254	8.4	A.U.	Sandstones	3.07 ± 0.34	8.67 ± 1.11	7	
TM 254	8.1	A.U.	Argil. sandst.	9.04 ± 1.13	6.55 ± 0.91	8	
TM 254	7.9	A.U.	Sandstones	6.89 ± 0.65	7.08 ± 0.80	9	
TM 254	7.3	A.U.	Sandstones	6.20 ± 0.83	7.39 ± 1.08	10	
							6.88 ± 0.40‡ (1.14)
TM 254	6.2	A.U.	Sandstones	6.34 ± 0.53	7.24 ± 0.75	11	
TM 254	6.1	A.U.	Sandstones	9.24 ± 2.40	6.50 ± 1.74	12	
TM 254	6	A.U.	Termite nest	6.47 ± 0.68	7.20 ± 0.88	13	
TM 254	6	A.U.	Termite nest	6.38 ± 0.91	7.23 ± 1.12	14	
TM 254	6	A.U.	Termite nest	6.00 ± 0.64	7.35 ± 0.91	15	
TM 254	5.9	A.U.	Sandstones	9.64 ± 2.29	6.42 ± 1.58	16	
TM 254	5.6	A.U.	Sandstones	5.13 ± 0.75	7.66 ± 1.21	17	
TM 254	5.4	A.U.	Sandstones	4.92 ± 1.04	7.74 ± 1.71	18	
							7.24 ± 0.38‡ (0.10)
TM 266	9	A.U.	Argil. sandst.	6.70 ± 1.27	7.14 ± 1.42	19	
TM 266	8.6	A.U.	Sandstones	7.07 ± 0.76	7.03 ± 0.61	20	
TM 266	8	A.U.	Sandstones	10.85 ± 1.46	6.19 ± 0.92	21	
TM 266	7.8	A.U.	Sandstones	7.32 ± 1.44	6.96 ± 1.44	22	
							6.83 ± 0.45‡ (0.22)
TM 266§	7.4	A.U.	Sandstones	—	—	—	
TM 266	6.7	A.U.	Sandstones	8.47 ± 1.56	6.68 ± 1.30	23	
TM 266	6.6	A.U.	Sandstones	3.82 ± 0.81	8.24 ± 1.81	24	
TM 266	6.5	A.U.	Sandstones	12.47 ± 2.27	5.92 ± 1.14	25	
TM 266	6.3	A.U.	Argil. sandst.	6.72 ± 0.43	7.13 ± 0.64	26	
TM 266	6.2	A.U.	Sandstones	5.55 ± 1.32	7.51 ± 1.84	27	
TM 266	6.1	A.U.	Sandstones	6.36 ± 0.63	7.24 ± 0.84	28	
TM 266	6	A.U.	Sandstones	7.17 ± 1.10	7.00 ± 1.16	29	
TM 266	5.8	A.U.	Sandstones	6.25 ± 0.73	7.27 ± 0.96	30	
TM 266	5.7	A.U.	Sandstones	4.72 ± 0.80	7.82 ± 1.42	31	
TM 266	5.4	A.U.	Sandstones	6.55 ± 0.48	7.18 ± 0.69	32	
							7.12 ± 0.31‡ (0.22)

The height baseline is the base of the TM 266 section. Below each group of samples is shown the mean age value calculated either with the weighed mean (†) or with the inverse-variance weighed mean (‡). KT, Koro Toro; KL, Kollé; KB, Kossom Bougoudi; TM, Toros-Menalla; Argil. sandst., Argillaceous sandstones; MSWD, mean square of weighted deviate; —, not applicable.

**A. bahrelghazali*.

§*Sahelanthropus tchadensis.*

The pelite relic authigenic $^{10}Be/^{9}Be$ age within the argillaceous sandstone containing the mandible of *Australopithecus bahrelghazali* (Abel, KT 12) sampled for calibration purpose indicates that the Koro Toro fossiliferous locality is at least 3.3 Ma old, an age that is in the range of the biochronological estimation by using the mammal evolutive degree (3, 4, 36). This new absolute dating constraint shows that *Australopithecus bahrelghazali* (Abel) was contemporaneous with *Australopithecus afarensis* and more particularly with Lucy from Awash valley, Ethiopia [≈3.18 ± 0.01 Ma (37, 38)].

The radiochronological data concerning *Sahelanthropus tchadensis* (Toumaï, TM 266) reported here is an important cornerstone both for establishing the earliest stages of hominid evolution and for new calibrations of the molecular clock. Thus, *Sahelanthropus tchadensis* testifies that the last divergence between chimps and humans is certainly not much more recent than 8 Ma, which is congruent with *Chororapithecus abyssinicus*, the new 10-Ma-old Ethiopian paleogorillid (39). With its mosaic of plesiomorphic and apomorphic characters *Sahelanthropus tchadensis*, the earliest known hominid (1, 2, 40), is probably very

close in time to this divergence contrary to the unlikely "provocative explanation," which recently suggested a "possible hybridization in the human-chimp lineage before finally separating less than 6.3 Ma" (41).

Materials and Methods

Beryllium Isotopes Measurements. Authigenic beryllium isotopes were extracted from dried and crushed sediments by using 0.04 M NH_2OH-HCl in a 25% acetic acid leaching solution (14). After removal of a 2-ml aliquot for ^{9}Be measurements, the remaining leachate was spiked with 300 μl of a 10^{-3} g g^{-1} ^{9}Be solution. For ^{10}Be measurements, this spiked solution was finally purified by solvent extractions of Be acetylacetonate in the presence of EDTA, followed by precipitations of $Be(OH)_2$ at pH 8.5 and rinsing. The final precipitate was dissolved in a few drops of HNO_3, dried, and heated at 1,000°C to obtain BeO.

^{9}Be concentrations were measured by graphite furnace atomic absorption spectrophotometry (at CEREGE on a Hitachi Z-8200) using Zeeman effect background correction. The reproducibility of standard addition absorptions and the fit of standard addition lines were then used to determine ^{9}Be uncertainties. ^{10}Be concentration was deduced from the spiked ^{10}Be/^{9}Be ratios measured by accelerator MS at the Tandetron facility in Gif/Yvette (France). The presented data were calibrated directly against the National Institute of Standards and Technology standard reference material 4325 by using the values recently determined by Nishiizumi *et al.* (33), which are a ^{10}Be/^{9}Be ratio of $(2.79 \pm 0.03) \times 10^{-11}$ and a ^{10}Be half-life of $(1.36 \pm 0.07) \times 10^6$ years. ^{10}Be uncertainties result from statistical uncertainties linked to the number of ^{10}Be events detected coupled to a 3% analytical uncertainty deduced from the reproducibility throughout the measurement sequences. Propagation of the ^{10}Be and ^{9}Be uncertainties ultimately determines the uncertainty linked to the ^{10}Be/^{9}Be ratio.

Age Calculations. The uncertainty assigned to individual ages results from the propagation of the uncertainty linked to the initial ^{10}Be/^{9}Be ratio (N_0), to the measured ^{10}Be/^{9}Be ratio and to the ^{10}Be half-life.

The uncertainty associated to the inverse-variance weighed mean ages depends of the mean square of weighed deviates (MSWD) value. Following McIntyre et *al* (42), the MSWD is equivalent to the χ^2 statistic divided by the number of degrees of freedom and compares the observed variability within the sample population to the expected variability defined by the analytical uncertainties of the measurements. An MSWD value of 1.0 indicates that analytical errors are as expected, whereas a value less than 1.0 indicates that the analytical error may be overestimated. Because all of the calculated MSWD were close or lower than 1.0, the uncertainty associated to the inverse-variance weighed mean ages σ_T is equal to $(1/\sum w_i)^{1/2}$, where w_i is the weighing factor $(1/\sigma_i^2)$ of each individual sample.

ACKNOWLEDGMENTS. We thank Profs. Paul Rene, Edouard Bard, and Robert Finkel for advice and discussions; Prof. Pierre Batteau for assistance in the statistical analysis; Dr. Baba El-Hadj Mallah (Centre National d'Appui de la Recherche); the French Army (Mission d'Assistance Militaire et Epervier); all the Mission Paléoanthropologique Franco-Tchadienne members; G. Florent and C. Noël for administrative guidance; and A. Bouzeghaia for artwork support. This manuscript benefited significantly from a thorough review by Francis H. Brown, Darryl Granger, and an anonymous reviewer. This work was supported by the Ministère Tchadien de l'Enseignement Supérieur et de la Recherche (l'Université de N'Djamena and the Centre National d'Appui de la Recherche), the Ministère Français des Affaires Etrangères (Ambassade de France à N'Djamena, Service de Coopération et d'Action Culturelle, projet Fonds de Solidarité Prioritaire and Direction de la Coopération Scientifique, Universitaire et de la Recherche, Paris), the Ministère Français de l'Education Nationale et de la Recherche (Centre National de la Recherche Scientifique, Environment et Climat du Passé: Histoire et Evolution, the Agence National de la Recherche, Université de Poitiers), Région Poitou Charentes, and the National Science Foundation Revealing Hominids Origins Initiative.

1. Brunet M, *et al.* (2002) A new hominid from the Upper Miocene of Chad, Central Africa. *Nature* 418:145–151.
2. Brunet M, *et al.* (2005) New material of the earliest hominid from the Upper Miocene of Chad. *Nature* 434:752–755.
3. Brunet M, *et al.* (1995) The first australopithecine 2500 kilometres west of the Rift Valley (Chad). *Nature* 378:273–275.
4. Brunet M, *et al.* (1996) Australopithecus bahrelghazali, une nouvelle espèce d'hominidé ancien de la région de Koro Toro (Tchad). *C R Acad Sci Paris* 322:907–913.
5. Vignaud P, *et al.* (2002) Geology and paleontology of the Upper Miocene Toros-Menalla hominid locality. *Nature* 418:152–155.
6. Deino AL, Tauxe L, Monaghan M, Hill A (2002) ^{40}Ar/^{39}Ar geochronology and paleomaognetic stratigraphy of the Lukeino and lower Chemeron Formations at Tabarin and Kapcheberek, Tugen Hills, Kenya. *J Hum Evol* 42:117–140.
7. MacDougall I, Feibel CS (2003) Numerical age control for the Miocene-Pliocene succession at Lothagam. *Lothagam the Dawn of Humanity in Eastern Africa*, eds Leakey MG, Harris JM (Columbia Univ Press, New York), pp 43–64.
8. Schuster M, *et al.* (2006) The age of the Sahara desert. *Science* 311:821.
9. Duringer P, *et al.* (2006) The first fungus gardens of Isoptera: Oldest evidence of symbiotic termite fungiculture (Miocene, Chad basin). *Naturwissenschaften* 93:610–615.
10. Duringer P, *et al.* (2007) New termite trace fossils: Galleries, nests and fungus combs from the Chad Basin of Africa (Upper Miocene–Lower Pliocene). *Palaeogeogr Palaeoclimatol Palaeoecol* 251:323–353.
11. Raisbeck GM, *et al.* (1981) Cosmogenic ^{10}Be/^{7}Be as a probe of atmospheric transport processes. *Geophys Res Lett* 8:1015–1018.
12. Measures CI, Edmond JM (1983) The geochemical cycle of ^{9}Be: A reconnaissance. *Earth Planet Sci Lett* 66:101–110.
13. Brown ET, *et al.* (1992) Continental inputs of beryllium to the oceans. *Earth Planet Sci Lett* 114:101–111.
14. Bourlès DL, Raisbeck GM, Yiou F (1989) ^{10}Be and ^{9}Be in marine sediments and their potential for dating. *Geochim Cosmochim Acta* 53:443–452.
15. Libby WF (1965) *Radiocarbon Dating* (Univ of Chicago Press, Chicago), 2nd Ed.
16. Henken-Mellies WU, *et al.* (1990) ^{10}Be and ^{9}Be in South Atlantic DSDP Site 519: Relation to geomagnetic reversals and to sediment composition. *Earth Planet Sci Lett* 98:267–276.
17. Yokoyama Y, Guichard F, Reyss JL, Nguyen Huu Van (1978) Oceanic residence times of dissolved beryllium and aluminium deduced from cosmogenic tracers ^{10}Be and ^{26}Al. *Science* 201:1016–1017.
18. Krishnaswami S, *et al.* (1982) ^{10}Be and Th isotopes in manganese nodules and adjacent sediments: nodules growth histories and nuclide behavior. *Earth Planet Sci Lett* 59:217–234.
19. Inoue T, Huang ZY, Imamura M, Tanaka S, Usui A (1983) ^{10}Be and ^{10}Be/^{9}Be in manganese nodules. *Geochim J* 17:307–312.
20. Sharma P, Somayajulu BLK (1982) ^{10}Be dating of large manganese nodules from world oceans. *Earth Planet Sci Lett* 59:235–244.
21. Kusakabe M, Ku TL (1984) Incorporation of Be isotopes and other trace metals into marine ferromanganese deposits. *Geochim Cosmochim Acta* 48:2187–2193.
22. Ku TL, *et al.* (1982) Constancy of oceanic deposition of ^{10}Be as recorded in ferromanganese crusts. *Nature* 299:240–242.
23. Von Blanckenburg F, O'Nions RK, Belshaw NS, Gibb A, Hein JR (1996) Global distribution of beryllium isotopes in deep ocean water as derived from Fe-Mn crusts. *Earth Planet Sci Lett* 141:213–226.
24. Ku TL, *et al.* (1990) Beryllium isotope distribution in western North Atlantic: A comparison to the Pacific. *Deep-Sea Res* 35:795–808.
25. Measures CI, *et al.* (1996) The distribution of ^{10}Be and ^{9}Be in the South Atlantic. *Deep-Sea Res* 43:987–1009.
26. Measures CI, Edmond JM (1982) Beryllium in the water column of the central North Pacific. *Nature* 297:51–53.
27. Sharma P, Mahannah R, Moore WS, Ku TL, Southon JR (1987) Transport of ^{10}Be and ^{9}Be in the ocean. *Earth Planet Sci Lett* 86:69–76.
28. Kusakabe M, *et al.* (1987) Distribution of ^{10}Be and ^{9}Be in the Pacific Ocean. *Earth Planet Sci Lett* 82:231–240.
29. Kusakabe M, *et al.* (1987) The distribution of ^{10}Be and ^{9}Be in the ocean water. *Nucl Inst and Meth* B29:306–310.
30. Kusakabe M, *et al.* (1991) Be isotopes in rivers/estuaries and their oceanic budgets. *Earth Planet Sci Lett* 102(3–4):265–276.
31. Graham IJ, Ditchburn RG, Whitehead NE (2001) Be isotope analysis of a 0–500 ka loess–paleosol sequence from Rangitatau East, New Zealand. *Quat Int* 76/77:29–42.
32. Schuster M, *et al.* (2005) Holocene Lake Mega-Chad paleoshorelines from space. *Quat Sci Rev* 24:1821–1827.
33. Nishiizumi K, *et al.* (2007) Absolute calibration of ^{10}Be AMS standards. *Nucl Instrum Methods B* 58:403–413.
34. Brunet M, *et al.* (1998) Tchad: Découverte d'une faune de Mammifères du Pliocène inférieur. *C R Acad Sci Paris* 326:153–158.
35. Brunet M, MPFT (2000) Chad: Discovery of a vertebrate fauna close to the Mio–Pliocene boundary. *J Vertebrate Palaeontol* 20:205–209.
36. Brunet M, *et al.* (1997) Tchad: Un nouveau site à Hominidés pliocène. *C R Acad Sci Paris* 324:341–345.
37. Johanson DC, White TD, Coppens Y (1978) A new species of the genus *Australopithecus* (Primates; Hominidae) from the Pliocene of eastern Africa. *Kirtlandia* 28:1–14.
38. Walter RC (1994) Age of Lucy and the first family: Single-crystal ^{40}Ar/^{39}Ar dating of the denen Dora and lower Kada Hadar member of the Hadar Formation, Ethiopia. *Geology* 22:6–10.
39. Suwa G, Kono RT, Katoh S, Asfaw B, Beyene Y (2007) A new species of great ape from the late Miocene epoch in Ethiopia. *Nature* 448:921–924.
40. Zollikofer CP, *et al.* (2005) Virtual cranial reconstruction of *Sahelanthropus tchadensis*. *Nature* 434:755–759.
41. Patterson N, Richter DJ, Gnerre S, Lander ES, Reich D (2006) Genetic evidence for complex speciation of humans and chimpanzees. *Nature* 441:1103–1108.
42. McIntyre GA, Brooks C, Compston W, Turek A (1966) The statistical assessment of Rb-Sr isochrones. *J Geophys Res* 71:5459–5468.